Journal of Engineering Science and Technology
9th EURECA 2017 Special Issue September (2018) 83 - 93

KAPUR/TSALLIS ENTROPY GUIDED SEGMENTATION OF PLASMODIUM SPECIES FROM THIN BLOOD SMEAR IMAGES

DEEPTI SURESH, SRI MADHAVA RAJA N., KIRTHINI GODWEENA A.*

Department of Electronics and Instrumentation Engineering, St. Joseph's College of Engineering, Rajiv Gandhi Road, Chennai 600119, India
*Corresponding Author: kirthini.888@gmail.com

Abstract

A well-known mosquito-borne transmissible sickness in humans, commonly named Malaria is majorly caused due to plasmodium species. In order to minimize the disease impact, it is necessary to identify the type of the species before initiating the treatment process. Exact identification of the Plasmodium species is advisable to treat the infected person with a specific anti-malarial drug. In this work, a scheme for image segmentation is proposed to extract the plasmodium species from thin blood smear images using famous entropy based procedures, such as Kapur / Tsallis function and Bat Algorithm (BA). Throughout the work, maximization of objective function is effected to drive the BA. The proposed methodology is validated with a qualitative and quantitative analysis. The results shows evidence that the, proposed approach seems to be is effective to extract the species from blood smear images.

Keywords: Bat algorithm, Entropy values, Evaluation, Plasmodium, Segmentation.

1. Introduction

In imaging discipline, image processing articulates a vital part in exploring and understanding the images from fields such as medical, navigation, automatic event detection, surveillance, environment modeling, pattern and texture recognition, and damage detection [1-4]. The development digital image based techniques and computation expertise has increased the potential of imaging discipline. Segmentation procedure, the pre-processing procedure allows to obtain prominent information from input image. Segmentation is judged as a key procedure for significant examination and elucidation of images [5-8].

In recent years, medical imaging and its processing have invited the research community due its significance. In this work, an endeavor is employed for segmenting images of blood smear, which are affected by malaria. The disease is a life threatening contagious disease borne by mosquitoes. Recently, Manickavasagam et al. [9] made a study on the comprehensive segmentation technique and also listed the existing anti-malarial drug for the Plasmodium species. Literature also offers methodology for handling blood smear images, which are Plasmodium infected [10, 11]. Even though many attempts are made on segmenting these, there is a scope of improving the efficacy of segmentation in early detection of pathology in the considered images.

In many instances, the image samples in RGB are subjected to segmentation by their gray scale. The effects of this procedure is obtained in a (0-255) color scale of gray. In this work, the colour images in RGB are converted into gray scale images and segmented using Kapur's and Tsalli's function using the BA.

In this attempt, the samples were obtained from the DPDx repository of the Centers for Disease Control and Prevention [12]. In this effort, BA is employed to solve the bi-level segmentation problem. The quality measures of image, such as MSE, RMSE, NAE, NCC, MD, SC, PSNR, AD, and SSIM were extracted [13-15]. In addition to this, statistical features, such as mean, median, standard deviation, sum and variance is extracted for the further analysis.

2. Materials and Methods

In this paper, image segmentation was carried out using well known entropy centered approaches, such as Tsallis and Kapur functions, since these methods are proven to be successful in segmenting in the literature.

2.1. Kapur's entropy

Kapur's method identifies the optimal threshold by entropy maximization of the histogram [16]. This entropy is expressed as;

$$J_{\max} = f_{kapur}(th) = \sum_{j=1}^{k} H_j^C \tag{1}$$

In general, each value of entropy is figured individually from a specific value of *th*. For multi-thresholding concerns, it is presented as

$$
\begin{aligned}
H_1^C &= \sum_{j=1}^{th_1} \frac{Ph_j^C}{\omega_0^C} \ln\left(\frac{Ph_j^C}{\omega_0^C}\right), \\
H_2^C &= \sum_{j=th_1+1}^{th_2} \frac{Ph_j^C}{\omega_1^C} \ln\left(\frac{Ph_j^C}{\omega_1^C}\right), \\
&\vdots \\
H_{k.}^C &\sum_{j=th_k+.1}^{L'} \frac{Ph_j^C}{\omega_{k-1}^C} \ln\left(\frac{Ph_j^C}{\omega_{K-1}^C}\right)
\end{aligned} \tag{2}
$$

where, Ph_j^C is the distribution of probability for various levels of intensity, 1 is assigned as value to *C* for different images in gray. The probability occurrence for various *k* levels are denoted by $\omega_0^C, \omega_1^C, ...\omega_{k-1}^C$. The BA driven search randomly amends the values of the threshold till J_{max} is attained.

2.2. Tsallis function

Initially, a combination of the BA and the TE is executed as a pre-processing technique. Customarily, to estimate of vagueness inside an image, entropy is used. Shannon's theory guaranteed that, if a bodily structure is parted as separate open sub-systems like '*U*' and '*V*' statistically, then the entropy value will be [17]:

$$S(U+V) = S(U) + S(V) \tag{3}$$

Then, TE will be:

$$S_q = \frac{1-\sum_{i=1}^{T}(p_i)^q}{q-1} \tag{4}$$

where, structure's possibility is represented *T* and entropic directory is signified by *q*=. Equation (2) forms Shannon-entropy when $q \to 1$.The final entropy is:

$$S_q(U+V) = S_q(U) + S_q(V) + (1-q).S_q(U).S_q(V) \tag{5}$$

TE provides optimal threshold for image. Let, image has *L*-gray values of range {0, 1, ...,*L*-1}, through likelihood allocation $p_i = p_0, p_1, ..., p_{L-1}$. TE is expressed as:

$$
\begin{aligned}
&f(T)=[T_1,T_2,...T_k]=argmax \\
&\left[S_q^U(T) + S_q^V(T) + ... + S_q^K(T) + (1-q).S_q^U(T).S_q^V(T)..S_q^K(T)\right]
\end{aligned} \tag{6}
$$

where

$$S_q^U(T) = \frac{1-\sum_{i=0}^{t_1-1}\left(\frac{Pi}{P^U}\right)^q}{q-1}, \; P^U = \sum_{i=0}^{t_1-1} Pi$$

$$S_q^V(T) = \frac{1-\sum_{i=t_1}^{t_2-1}\left(\frac{Pi}{P^V}\right)^q}{q-1}, \; P^V = \sum_{i=t_1}^{t_2-1} Pi$$

$$S_q^K(T) = \frac{1-\sum_{i=t_k}^{L-1}\left(\frac{Pi}{P^K}\right)^q}{q-1}, \; P^K = \sum_{i=t_k}^{L_2-1} Pi$$

In this practice, optimal threshold value T is obtained by maximizing $f(T)$. Implemented effort finds the arbitrary values of the T based on the heuristic search by the SGO algorithm. The threshold level is assigned as T =3 [18-20], with probabilities P^A, P^B, and P^C. The heuristic search continuously explores the gray level thresholds of the chosen MRI threshold and computes the value of $f(T)$. This process continues till the search converges with a maximized value of the $f(T)$ or till the maximum iteration value is reached.

2.3. Bat algorithm (BA)

The BA was firstly proposed by imitating the hunting actions of microbats [21]. BA consists of three mathematical expressions such as i) velocity, ii) position and iii) frequency updates as described in the following equations [22]:

$$V_i^{(t+1)} = V_i^{(t)} + (X_i^{(t)} - Gbest).F_i \tag{7}$$

$$X_i^{(t+1)} = X_i^{(t)} + V_i^{(t+1)} \tag{8}$$

$$F_i = F_{\min} + (F_{\max} - F_{\min}).\beta^1 \tag{9}$$

where, $V_i^{(t+1)}$ symbolize the velocity and X_i^{t+1} denotes the position of the bat, F_{min} is the least frequency and F_{max} is highest frequency.

From Eq. (7), it is noted that, velocity updating depends primarily on the renewal of the frequency. During the heuristic analysis, a different result for every bat is obtained based on the relation:

$$X_{new} = X_{old} + \varepsilon A^t \tag{10}$$

where ε= arbitrary value lies in the range [-1,1] and A is represents the intensity of discharged sound during the investigation of a new "area" (set of locations leading to a set of results).

The numerical illustrations for intensity modification are shown below:

$$A_i^{(t+1)} = \alpha_1 A_i^{(t)} \tag{11}$$

$$r_i^{(t+1)} = r_i(0)[1 - \exp(-\gamma_1 t)] \tag{12}$$

In this work, CBA discussed in [15] is considered with the following parameters: Total bats = 30; exploration dimension = 2; iterations = 250; ending criteria = $J(t)_{max}$; β = [0,1], the frequency vector constant; ε is an arbitrary value [-1,1]; A_0 takes 10 and A_{min} is fixed as 1 (which declines in steps of 0.1); α^1 = γ^1=0.65.

3. Results and Discussions

The results obtained with the suggested methodology is presented in this section. All the simulation works are carried using Matlab 2012a on an Intel Core i3 CPU, 4 Giga Byte RAM running on Windows 8. This multi-level thresholding problem determines optimal threshold values in the threshold choice range of [0, L−1] that orients to maximizing a fitness function J_{max}. In this work, exploration dimension with optimization constraint is chosen as two (bi-level thresholding). For every

image and its individual threshold value, the process of segmentation is repeated 10 times and the trials mean value is chosen to be the optimum value. Figure 1 shows the flow chart of the automated disease prediction procedure. In this paper, plasmodium species such as P.F, P.M, P.K, P.V and P.O available in DPDx [12] is considered.

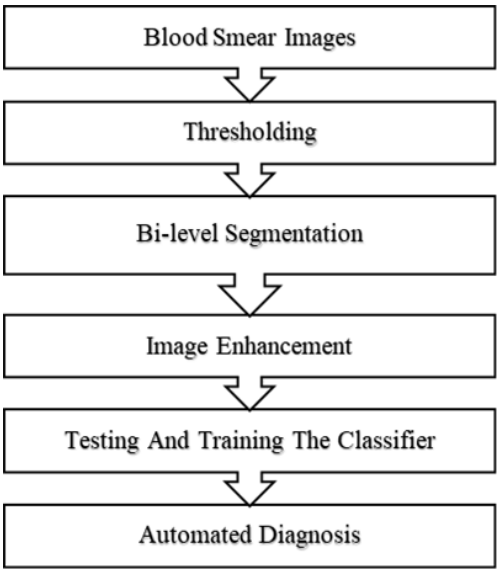

Fig. 1. Automated disease prediction procedure.

Before the segmentation process, to maintain consistency, all the 300 x 300 blood smear images are resized as a standard 256×256 images. In general, the data space, the distribution of gray level between 0 to 255, while the histogram in RGB has a higher range of pixels with a data space accounting to $[0, 255]^3$ [23]. Henceforth, in this attempt, gray level image based segmentation is adopted. Initially Kapur based bi-level thresholding method is verified on the dataset as shown in Table 1. The above discussed procedure is continued for the same images by Tsallis function. The segmentation process is repetitive for 20 times, for all the images individually and the mean is obtained for analysis.

The discussed procedure for two levels of threshold is able to distinguish the region of interest (plasmodium species) from its background without any loss in information. The qualitative measure of the segmentation procedure is assessed using the known image quality measures, such as RMSE, MSE, NCC, PSNR and AD [13] and also with SSIM [14]. Along with these procedures, the time taken by the CPU to identify the optimal threshold is also considered to assess the performance of Kapur and Tsallis based segmentation.

For increasing the visibility of plasmodium, the image segmented (SI) is then its inverted (IM) and the geometric features of the images such as, mean, median, standard deviation, sum and variance is extracted for further analysis.

Table 1. Microscope image and its histogram.

Subject	Image	Histogram
P. F	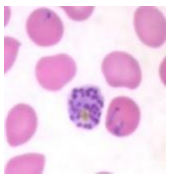	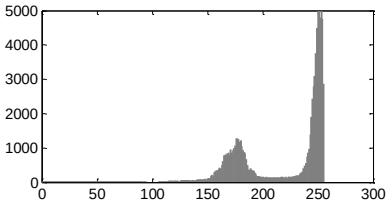
P. K	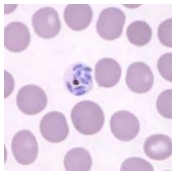	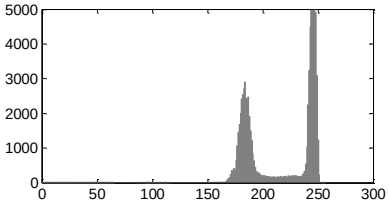
P. M	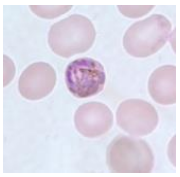	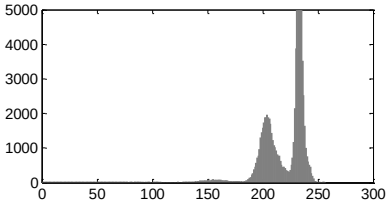
P. O	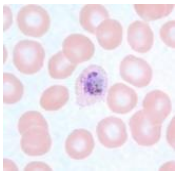	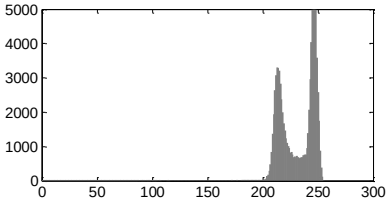
P. V	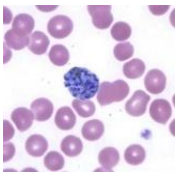	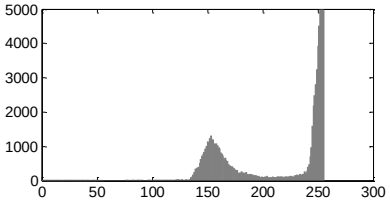

Table 2 shows SI and IM obtained with Kapur and Tsallis function. Table 3 presents the quantitative measures obtained in this study. Table 4 and 5 presents the qualitative measure values and Table 6 presents the statistical parameters of the image computed using the IM. From this result, one can observe that, Tsalli's function offers better results compared with the Kapur's function in all the cases. The results confirm that, the proposed segmentation procedure can be used to segment microscopic images, and in future, the extracted features can be considered for the automated classification and drug discovery process.

Table 2. Segmented and inverted image for the analysis.

Image	Kapur		Tsallis	
	SI	NI	SI	IM
P.F		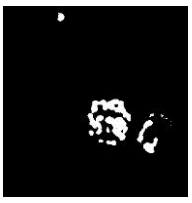		
P.K		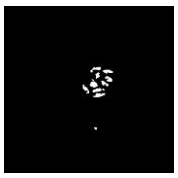		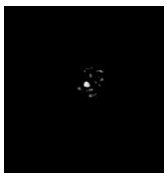
P.M				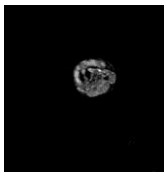
P.O		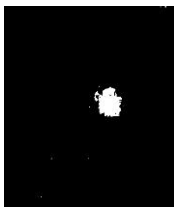		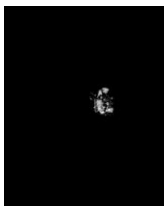
P.V		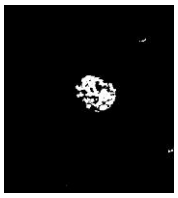		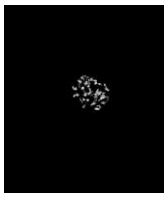

Table 3. Quantitative Measures analysis.

Image	OF		OT		CPU time (sec)	
	Kapur	Tsallis	Kapur	Tsallis	Kapur	Tsallis
P.F	10.3978	0.7903	129,255	131,255	12.4017	12.2594
P.K	10.4974	0.8407	148,255	149,255	17.0105	16.2995
P.M	9.0181	0.8699	170,255	160,255	15.6002	17.4016
P.O	9.0087	0.8703	199,255	191,255	14.0002	15.1096
P.V	9.1993	0.8102	140,255	129,255	16.1098	16.7927

Table 4. Quantitative measures with Kapur's function.

Image	P.F	P.K	P.M	P.O	P.V
MSE	2.67E+03	2.32E+03	2.15E+03	1.13E+03	3.73E+03
RMSE	51.6809	48.1195	46.4029	33.6403	61.0425
NAE	0.1587	0.1697	0.1688	0.1081	0.1961
NCC	1.1044	1.1416	1.1184	1.0868	1.1351
AD	-27.0488	-35.0538	-25.2011	-20.5062	-37.7511
MD	152	164	187	201	134
PSNR	13.8642	14.4844	14.7999	17.5936	12.4182
SSIM	0.7922	0.7513	0.7806	0.837	0.7413

Table 5. Quantitative measures with Tsalli's function.

Image	P.F	P.K	P.M	P.O	P.V
MSE	2.30e+03	1.91e+03	2.04e+03	779.1413	3.67e+03
RMSE	48.8572	46.0028	36.1278	28.7234	61.616
NAE	0.1482	0.1684	0.146	0.1015	0.1951
NCC	1.1193	1.145	1.1387	1.0958	1.1532
AD	-33.5726	-37.4539	-32.6197	-23.9182	-40.1661
MD	138	140	154	183	123
PSNR	13.5237	15.6895	16.2223	18.2705	13.4825
SSIM	0.7792	0.7486	0.7685	0.8316	0.7351

Table 6. Image features with Kapur's and Tsalli's function.

Image		P.F	P.K	P.M	P.O	P.V
Mean	Kapur	247.21	253.15	245.17	251.57	250.08
	Tsallis	252.64	254.54	251.58	253.97	253.49
Median	Kapur	255	255	255	255	255
	Tsallis	255	255	255	255	255
Standard deviation	Kapur	43.18	21.13	48.6	29.03	34.53
	Tsallis	16.88	7.393	17.95	11.11	13.64
Sum	Kapur	1.69E+08	4.13E+07	3.23E+07	7.68E+07	1.27E+08
	Tsallis	3.67E+07	5.02E+06	2.99E+07	1.21E+07	1.66E+07
Variance	Kapur	1.89E+03	1.64E+03	2.37E+03	8.45E+02	1.29E+03
	Tsallis	2.84E+02	54.6708	3.25E+02	1.25E+02	1.84E+02

4. Conclusions

In this work, an attempt to segment all the three channel RGB of the thin blood smear images with Kapur and Tsallis function using BA. Maximization of entropy function is preferred as the aim of the work. The justification of segmentation oriented heuristic procedure is tested on 256×256 sized microscopic images. The qualitative measures, quantitative measures and image features are extracted using existing methods from the literature. The usage of Bat algorithm has considerably improved the segmentation efficiency in terms of detecting the vague pixels, which contribute for identifying the prognosis of the disease in early stages. From this study, the observations are conceived as, the Tsallis' function delivers better result in comparison with the Kapur. In future, the segmented image will allow to train and test the classifier for an improved automated diagnostic relevance for disease detection.

Nomenclatures

$A_{0,}\ A_{min}$	Intensity levels
F_{max}	Highest frequency
F_{min}	Least frequency
$J(t)_{max}$	Ending criteria
J_{max}	entropy
k	Levels
L	Gray values
Ph_j^C	Distribution of probability for various levels of intensity
q	Entropic directory
T	Structure's possibility
U, V	Open sub-systems
$V_i^{(t+1)}$	Velocity
X_i^{t+1}	Position of the bat,

Greek Symbols

β	Frequency vector constant
ε	Arbitrary value
ω_0^C	Probability occurrence

Abbreviations

AD	Average Difference
BA	Bat Algorithm
CBA	Chaotic Bat Algorithm
DPDx	Parasite Image Library
IM	inverted
MSE	Mean Square Error
NCC	Normalised Cross Correlation
P.F	P. Falciparum
P.K	P. Knowlesi
P.M	P. Malariae
P.O	P. Ovale
P.V	P. Vivax,
RGB	Red Green Blue channel
RMSE	Root Mean Square Error
SGO	Social Group Optimization
SI	Image Segmented
SSI	Structural Similarity Index Matrix
TE	Optimal Threshold for an image

References

1. Tuba, M. (2014). Multilevel image thresholding by nature-inspired algorithms: A short review. *Computer Science Journal of Moldova*, 22(3), 318-338.

2. Raja, N.S.M.; Rajinikanth, V.; and Latha, K. (2014). Otsu based optimal multilevel image thresholding using firefly algorithm. *Modelling and Simulation in Engineering*, Vol. 2014, Article ID 794574, 17 pages.
3. Rajinikanth, V.; and Couceiro, M.S. (2015). Optimal multilevel image threshold selection using a novel objective function. *Advances in Intelligent Systems and Computing*, 340, 177-186.
4. Rajinikanth, V.; Raja, N.S.M.; and Kamalanand, K. (2017). Firefly algorithm assisted segmentation of tumor from brain MRI using Tsallis function and Markov random field. *Journal of Control Engineering and Applied Informatics*, 19(3), 97-106.
5. Manic, K.S.; Priya, R.K.; and Rajinikanth, V. (2016). Image multithresholding based on Kapur/Tsallis entropy and firefly algorithm. *Indian Journal of Science and Technology*, 9(12), 1-6.
6. Raja, N.S.M.; Fernandes, S.L.; Dey, N.; Satapathy, S.C.; and Rajinikanth, V. (2018). Contrast enhanced medical MRI evaluation using Tsallis entropy and region growing segmentation. *Journal of Ambient Intelligence and Humanized Computing*, 1-12.
7. Raja, N.S.M.; Rajinikanth, V.; Fernandes, S.L.; and Satapathy, S.C. (2017). Contrast enhanced medical MRI evaluation using Kapur's entropy and hidden Markov random field. *Journal of Medical Imaging and Health Informatics*. 7(8), 1825-1829.
8. Rajinikanth, V.; Satapathy, S.C.; Fernandes, S.L.; and Nachiappan, S. (2017). Entropy based segmentation of tumor from brain MR images - A study with teaching learning based optimization. *Pattern Recognition Letters*, 94, 87-95.
9. Manickavasagam, K.; Sutha, S.; and Kamalanand, K. (2014). An automated system based on 2d empirical mode decomposition and k-means clustering for classification of Plasmodium species in thin blood smear images. *BMC Infectious Diseases*: 14(Suppl 3):P13.
10. Manickavasagam, K.; Sutha, S.; and Kamalanand, K. (2014). Development of systems for classification of different plasmodium species in thin blood smear microscopic images. *Journal of Advanced Microscopy Research*, 9(2), 86-92.
11. Balan, N.S.; Kumar, A.S.; Raja, N.S.M.; and Rajinikanth, V. (2016). Optimal multilevel image thresholding to improve the visibility of plasmodium sp. in blood smear images. *Advances in Intelligent Systems and Computing*, 397, 563-571.
12. Parasite Image Library: Malaria (2009). Retrieved October 5, 2017, from http://www.dpd.cdc.gov/dpdx/HTML/ ImageLibrary/Malaria_il.htm
13. Grgic, S.; Grgic, M.; and Mrak, M. (2004). Reliability of objective picture quality measures. *Journal of Electrical Engineering*, 55(1-2), 3-10.
14. Wang, Z.; Bovik, A.C.; Sheikh, H.R.; and Simoncelli, E.P. (2004). Image quality assessment: From error visibility to structural similarity. *IEEE Transactions on Image Processing*, 13(4), 600-612.
15. Satapathy, S.C.; Raja, N.S.M.; Rajinikanth, V.; Ashour, A.S.; and Dey, N. (2016). Multi-level image thresholding using Otsu and chaotic bat algorithm. *Neural Computing and Applications*, 29(12), 1285-1307.

16. Kapur, J.N.; Sahoo, P.K.; and Wong, A.K.C. (1985). A new method for gray-level picture thresholding using the entropy of the histogram. *Computer Vision, Graphics, and Image Processing*, 29(3), 273-285.
17. Tsallis, C. (1988). Possible generalization of Boltzmann-Gibbs statistics. *Journal of Statistical Physics*, 52(1-2), 479-487.
18. Rajinikanth, V.; Satapathy, S.C.; Fernandes, S.L.; and Nachiappan, S. (2017). Entropy based segmentation of tumor from brain MR images - A study with teaching learning based optimization. *Pattern Recognition Letters*, 94, 87-95.
19. Rajinikanth, V.; and Satapathy, S.C. (2018). Segmentation of ischemic stroke lesion in brain MRI based on social group optimization and fuzzy-Tsallis entropy. *Arabian Journal for Science and Engineering*, 43(8), 4365-4378.
20. Dey, N.; Rajinikanth, V.; Ashour, A.S.; and Tavares, J.M.R.S. (2018). Social group optimization supported segmentation and evaluation of skin melanoma images. *Symmetry*, 10(2), 51.
21. Yang, X.-S.; and He, X. (2013). Bat algorithm: literature review and applications. Int J Bio-Inspired Comput., 15(3), 141-149.
22. Yang, X.-S. (2008). *Nature-inspired metaheuristic algorithms* (2nd Edn.) Luniver Press, Frome, BA11 6TT, United Kingdom .
23. Rajinikanth V.; and Couceiro, M.S. (2015). RGB histogram based color image segmentation using firefly algorithm. *Procedia Computer Science*, 46, 1449-1457.